Supporting Information

Nanodenitrification with Bimetallic Nanoparticles Confined in N-doped Mesoporous Carbon

Jing Wang, Wei Teng, Lan Ling, Jianwei Fan, Wei-xian Zhang* and Zilong Deng*

State Key Laboratory for Pollution Control

School of Environmental Science and Engineering

Tongji University

1239 Siping Road

Shanghai, 200092 China

*Corresponding Authors

E-mail: zhangwx@tongji.edu.cn. Tel: +86-21-65985885.

zilongdeng@tongji.edu.cn

Contents:

Supporting information has 29 pages including Fig. S1- S22 and Table S1-S2.

concentrations (0, 50, 100, 150, 200 mg N/L). (scan rates of CV and polarization curves were 20 and 10 mV/s, respectively)

Fig. S15. Polarization curves before and after 5,000 CV cycles (a) and 10-month storage under ambient conditions (b). (scan rates of CV and polarization curves were 20 and 10 mV/s, respectively)

Fig. S16. HAADF image and STEM-XEDS elemental mappings of Cu-Pd@N-OMC-600 after denitrification process.

Fig. S17. TEM image of Cu-Pd@N-OMC-600 after denitrification process.

Fig. S18. Cu 2p XPS spectrum of Cu-Pd@N-OMC-600 after denitrification process.

Fig. S19. Pd 3d XPS spectrum of Cu-Pd@N-OMC-600 after denitrification process.

Fig. S20. Effect of pH on nitrate removal and N_2 selectivity using Cu-Pd@N-OMC-600 as electrode. (100 mg N/L of nitrate, 0.1 M Na_2SO_4, 20 h)

Fig. S21. Product distribution of nitrate reduction from eutrophic water (from a polluted campus pond in Tongji Universitys, Shanghai) on Cu-Pd@N-OMC-600 versus reaction time. (20 mL 50 mg N/L of nitrate, 10 h)

Fig. S22. Effect of eutrophic water volume on nitrate removal, N_2 selectivity and energy utilization efficiency using Cu-Pd@N-OMC-600 as electrode. (50 mg N/L of nitrate, 10 h)

Table S1. Comparison of nitrate reduction performance among published works.

Table S2. The quality analysis of eutrophic water from nitrate contaminated pond in Tongji University, Shanghai.

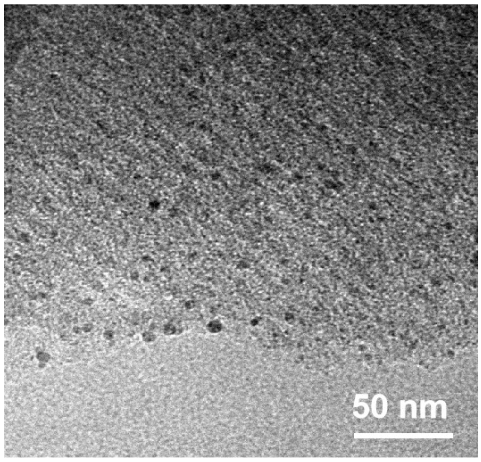

Fig. S1. TEM image of Cu-Pd@N-OMC-400.

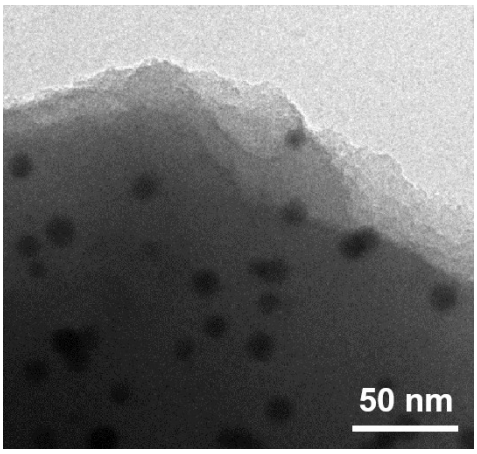

Fig. S2. TEM image of Cu-Pd@N-OMC-800.

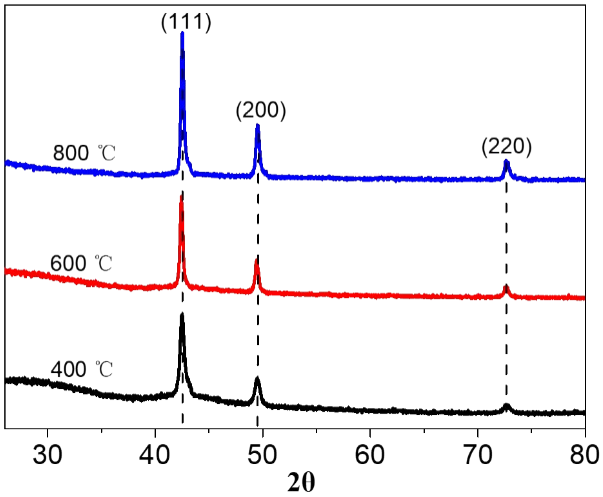

Fig. S3. XRD patterns of Cu-Pd@N-OMC pyrolyzed at 400, 600, and 800°C.

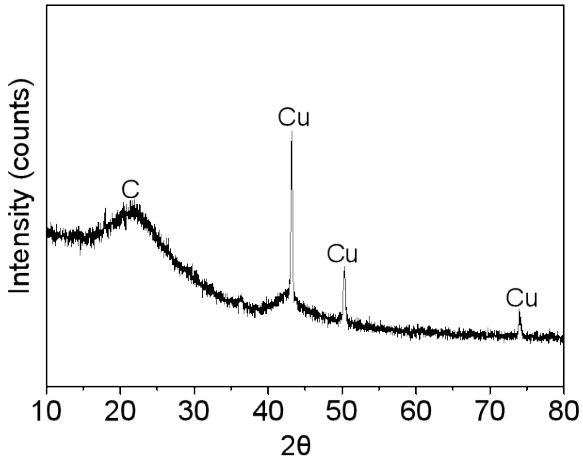

Fig.S4. XRD spectrum of Cu-Pd@OMC-600.

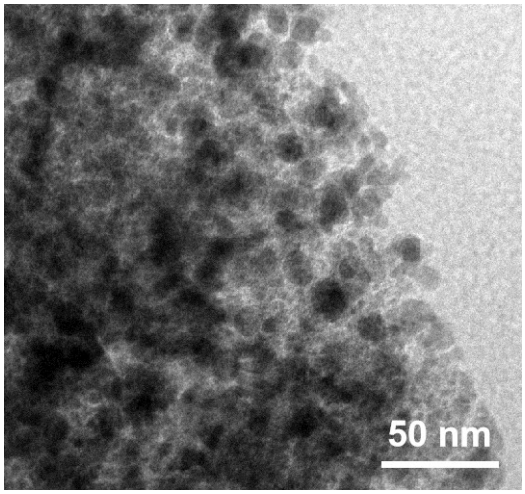

Fig. S5. TEM image of Cu-Pd@OMC-600.

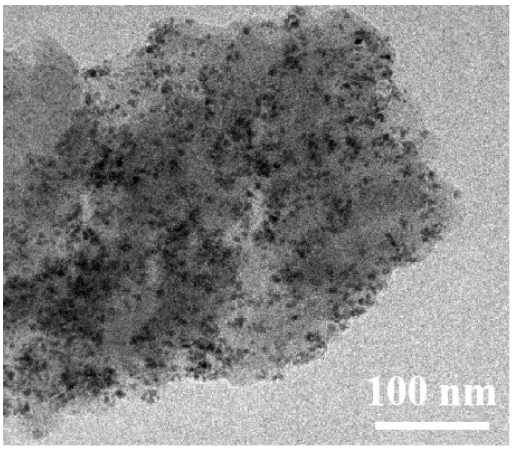

Fig.S6. TEM image of N-Cu-Pd-600.

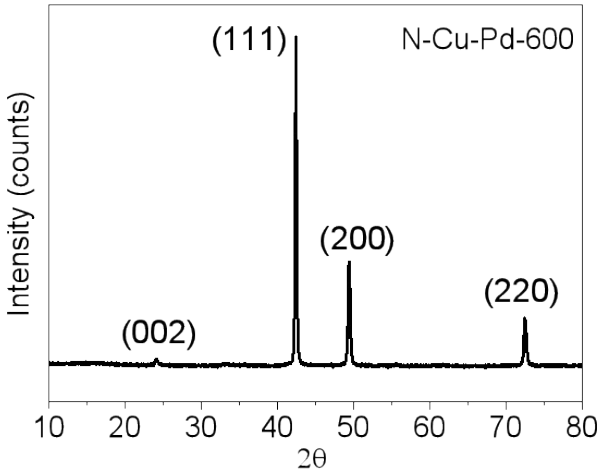

Fig.S7. XRD spectrum of N-Cu-Pd-600.

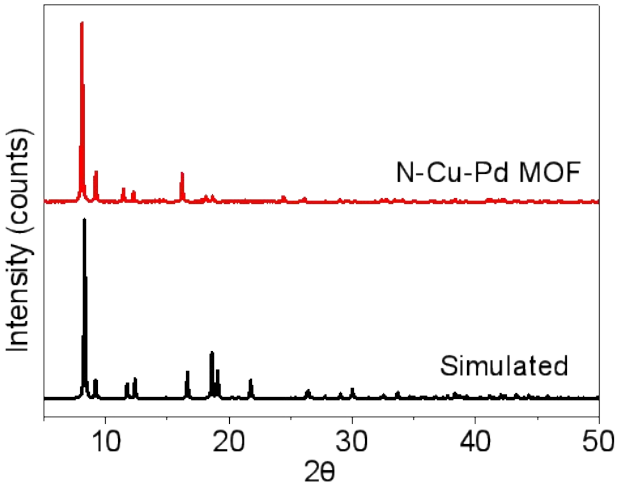

Fig. S8. XRD spectra of N-Cu-Pd MOFs.

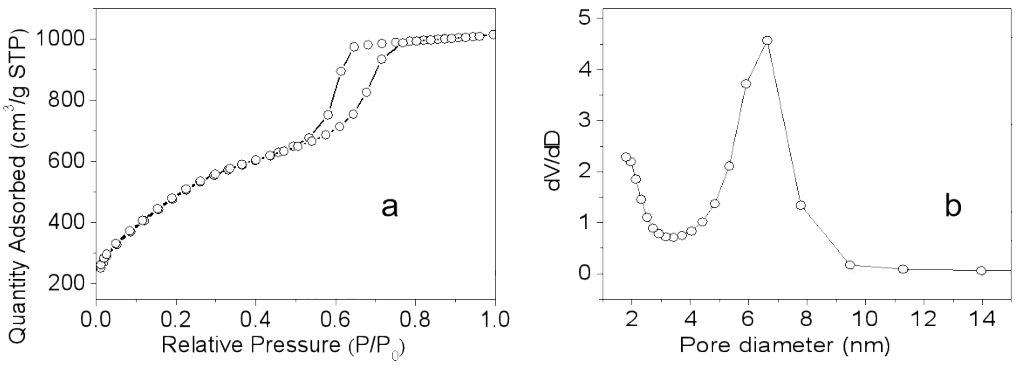

Fig. S9. (a) N_2 adsorption-desorption isotherm and (b) pore size distribution of ordered mesoporous carbon (OMC).

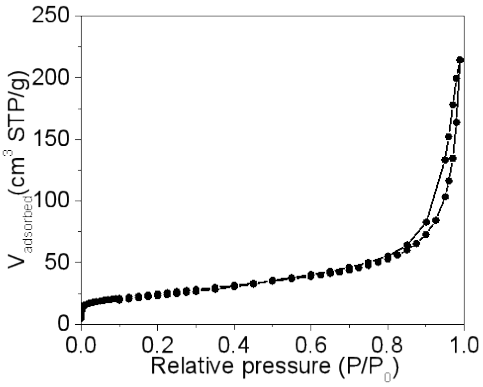

Fig. S10. N_2 adsorption-desorption isotherm of N-Cu-Pd MOFs.

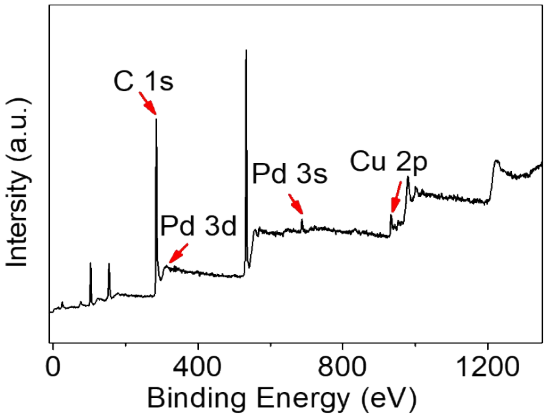

Fig. S11. The full XPS survey spectrum of Cu-Pd@N-OMC-600.

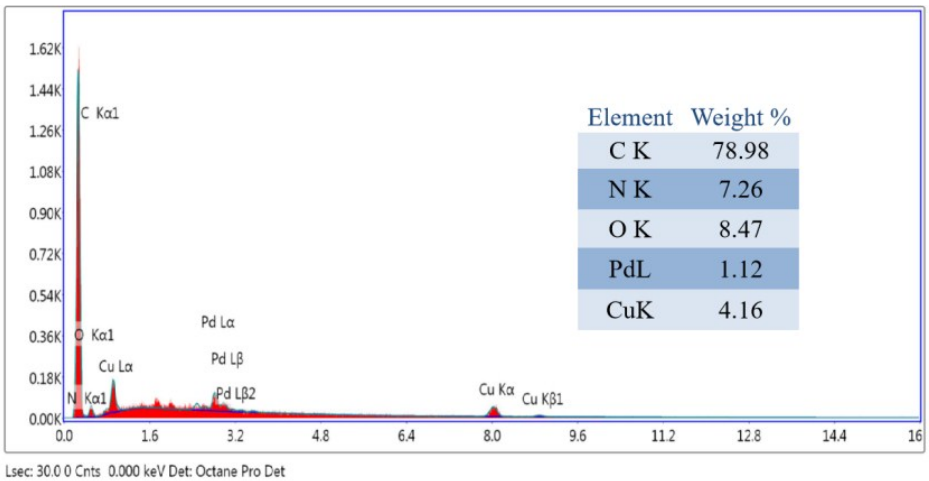

Element	Weight %
C K	78.98
N K	7.26
O K	8.47
PdL	1.12
CuK	4.16

Fig. S12. X-ray energy-dispersive spectroscopy (XEDS) of Cu-Pd@N-OMC-600.

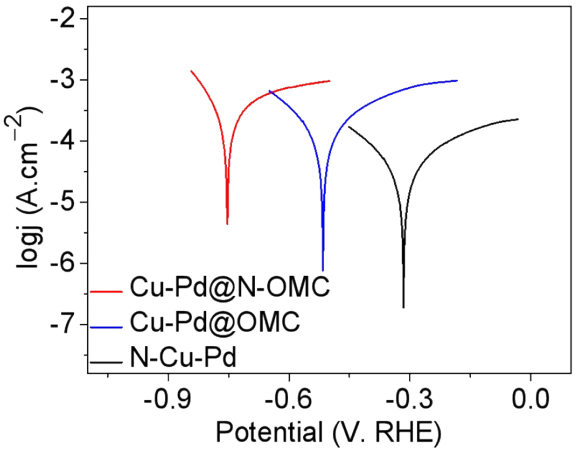

Fig. S13. Tafel plots of Cu-Pd@N-OMC-600, Cu-Pd@OMC-600 and N-Cu-Pd-600 (100 mg N/L nitrate, 0.1 M Na_2SO_4).

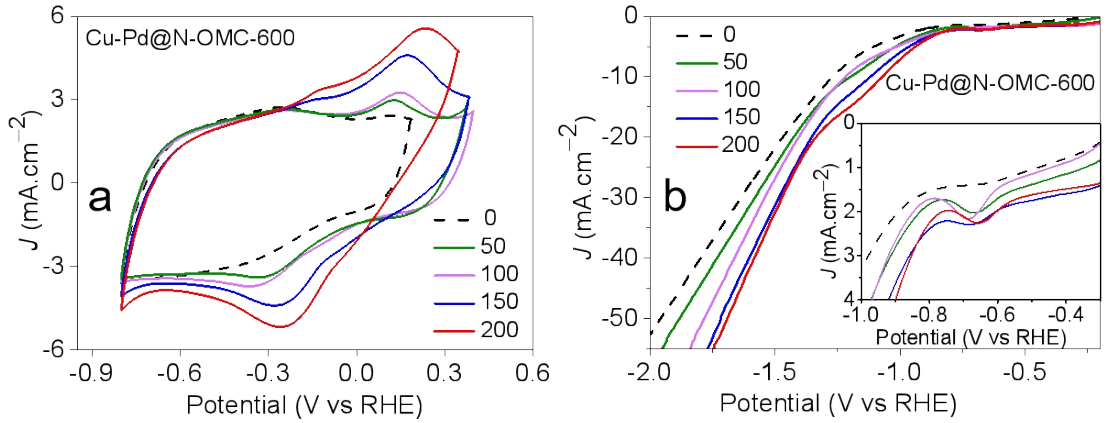

Fig. S14. (a) CV and (b) polarization curves on Cu-Pd@N-OMC-600 with varied nitrate concentrations (0, 50, 100, 150, 200 mg N/L). (scan rates of CV and polarization curve were 20 and 10 mV/s, respectively)

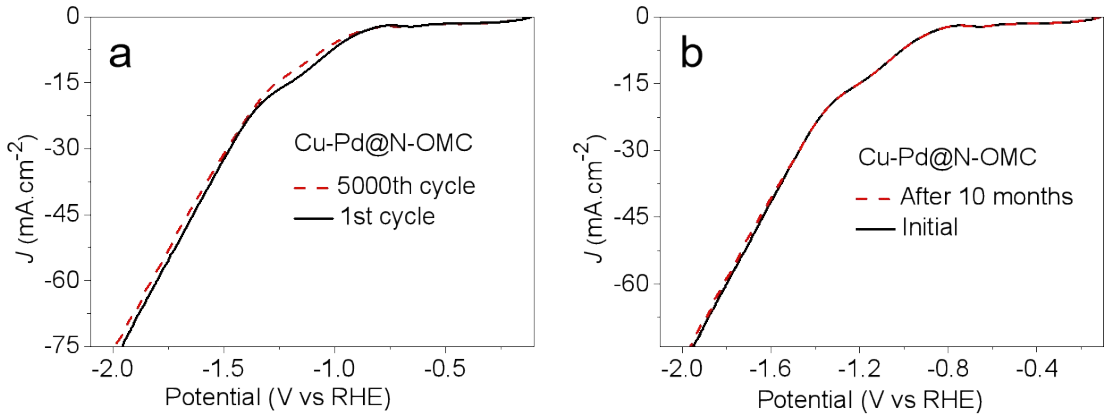

Fig. S15. Polarization curves of Cu-Pd@N-OMC-600 before and after 5,000 CV cycles (a) and 10-month storage under ambient conditions (b). (scan rates of CV and polarization curves were 20 and 10 mV/s, respectively)

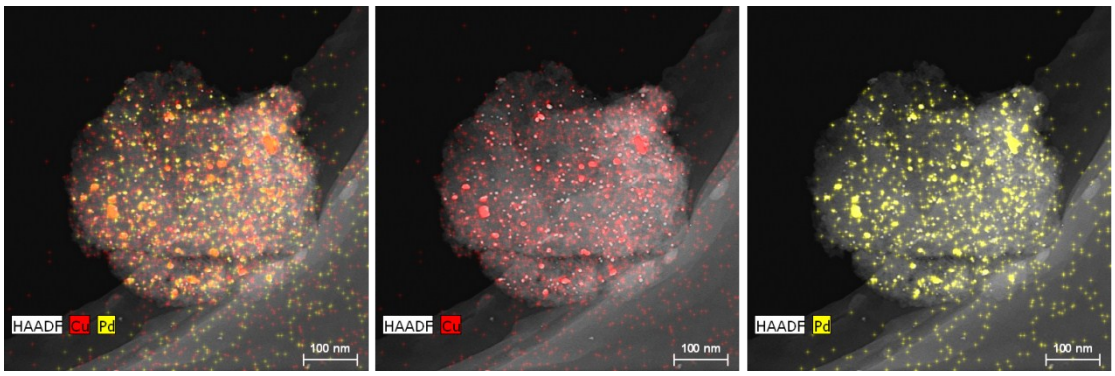

Fig. S16. HAADF image and STEM-XEDS elemental mappings of Cu-Pd@N-OMC-600 after denitrification process.

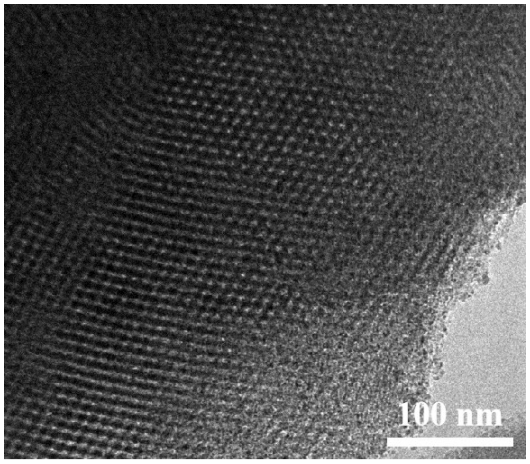

Fig. S17. TEM of Cu-Pd@N-OMC-600 after denitrification process.

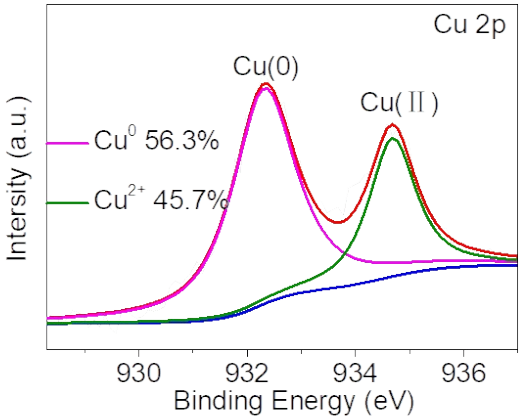

Fig. S18. Cu 2p XPS spectrum of Cu-Pd@N-OMC-600 after denitrification process.

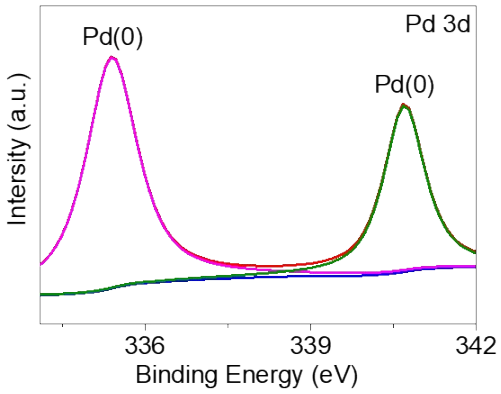

Fig. S19. Pd 3d XPS spectrum of Cu-Pd@N-OMC-600 after denitrification process.

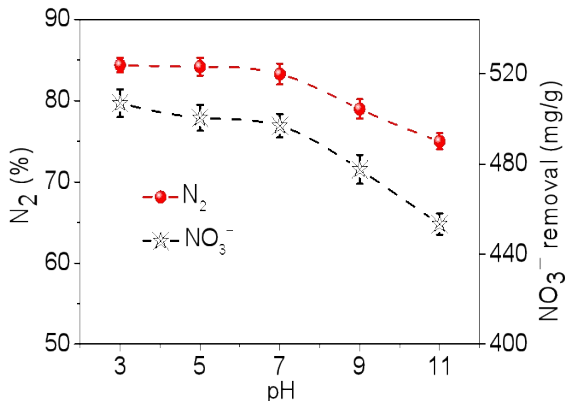

Fig. S20. Effect of pH on nitrate removal and N_2 selectivity using Cu-Pd@N-OMC-600 as electrode. (100 mg N/L of nitrate, 0.1 M Na_2SO_4, 20 h)

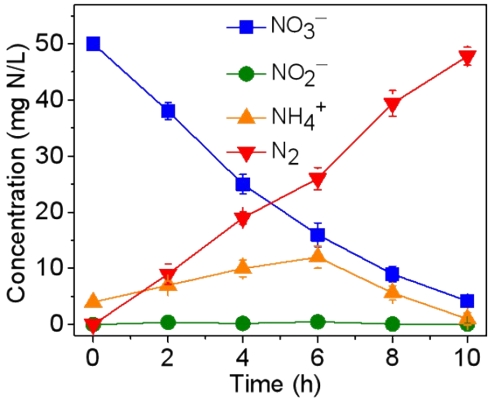

Fig. S21. Product distribution of nitrate reduction from eutrophic water (from a polluted campus pond in Tongji University, Shanghai) on Cu-Pd@N-OMC-600 versus reaction time. (20 mL 50 mg N/L of nitrate, 10 h)

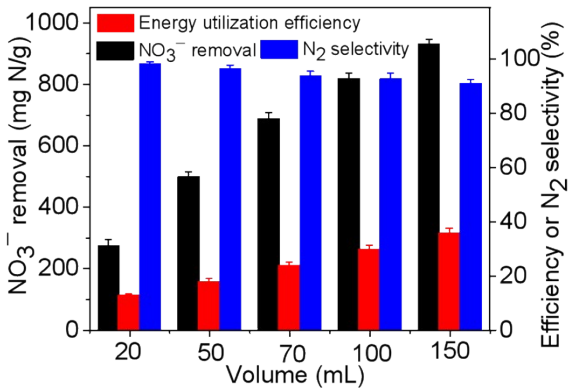

Fig. S22. The effect of eutrophic water volume on nitrate removal, N_2 selectivity and energy utilization efficiency using Cu-Pd@N-OMC-600 as electrode. (50 mg N/L of nitrate, 10 h)

Table S1. Comparison of nitrate reduction performance among published works.

Materials	Nitrate concentration (mg N/L)	NO_3^- Removal (%)	N_2 selectivity (%)	Ref.
Pd-Cu/TiO_2	100	90	76	Gao et al., 2003 [4]
Pd-Cu/AC	100	74	51.3	Trawczynski et al., 2011 [5]
Pd-Cu/Al_2O_3	100	100	74	Sa et al., 2005 [6]
Cu/Pd@OMC	3000	28.7	74	Fan et al., 2017 [7]
Pd-Cu/Hematite	30	96.4	73	Sungyoon et al., 2014 [8]
Pd/Sn	110	96	85	Wang et al., 2006 [9]
Pd_xCu_y@N-pC	100	95	80	Chen et al., 2018 [10]
nZVI@OMC	50	65	74	Teng et al., 2017 [11]
Cu-Pd@N-OMC-600	50	94	98.4	Our work

Table S2. The quality analysis of eutrophic water from nitrate contaminated pond in Tongji University, Shanghai.

Item	Value
NO_3^--N	15.8 mg/L
NO_2^--N	0.1 mg N/L
NH^{4+}-N	4.1 mg N/L
TN	20.0 mg/L
Na^+	53.2 mg/L
Ca^{2+}	46.9 mg/L
Mg^{2+}	20.9 mg/L
CO_3^{2-}	38.5 m/L
SO_4^{2-}	68.7 m/L
Cl^-	44.6 mg/L
S^{2-}	54.6 mg/L
P	1.7 mg/L
COD	43.9mg/L
pH	7.2

REFERENCES

1 R. V. Jagadeesh, K. Murugesan, A. S. Alshammari, H. Neumann, M. M. Pohl, J. Radnik and M. Beller, MOF-derived cobalt nanoparticles catalyze a general synthesis of amines, Science, 2017, **358**, 326-332.

2 M. Duca and M. T. M. Koper, Powering denitrification: the perspectives of electrocatalytic nitrate reduction, Energ. Environ. Sci., 2012, **5**, 9726-9742.

3 J. Martínez, A. Ortiz and I. Ortiz, State-of-the-art and perspectives of the catalytic and electrocatalytic reduction of aqueous nitrates, Appl. Catal. B Environ., 2017, **207**, 42-59.

4 W. Gao, N. Guan, J. Chen, X. Guan, R. Jin, H. Zeng, Z. Liu, F. Zhang, Titania supported Pd-Cu bimetallic catalyst for the reduction of nitrate in drinking water. *Appl. Catal. B Environ.* 2003, **46**, 341-351.

5 J. Trawczynski, P. Gheek, J. Okal, M. Zawadzki, M. J. Ilan Gomez, Reduction of nitrate on active carbon supported Pd-Cu catalysts. *Appl. Catal. A Gen.,* 2011, **409**, 39-47.

6 J. Sa, S. Gross, H. Vinek, Effect of the reducing step on the properties of Pd-Cu bimetallic catalysts used for denitration. *Appl. Catal. A Gen.,* 2005, **294**, 226-234.

7 Fan, H. Xu, M. Lv, J. Wang, W. Teng, X. Ran, X. Gou, X. Wang, Y. Sun, J. Yang, Mesoporous carbon confined palladium-copper alloy composites for high performance nitrogen selective nitrate reduction electrocatalysis. *New J. Chem*., 2017, **41**, 2349-2357.

8 J. Sungyoon, B. Sungjun and L. Woojin, Development of Pd-Cu/hematite catalyst for selective

nitrate reduction, Environ. Sci. Technol., 2014, **48**, 9651-9658.

9 Y. Wang, J. Qu, R. Wu and P. Lei, The electrocatalytic reduction of nitrate in water on Pd/Sn-modified activated carbon fiber electrode, Water Res., 2006, **40**, 1224-1232.

10 M. Chen, H. Wang, Y. Zhao, W. Luo, L. Li, Z. Bian, L. Wang, W. Jiang and J. Yang, Achieving high-performance nitrate electrocatalysis with PdCu nanoparticles confined in nitrogen-doped carbon coralline, Nanoscale, 2018, **10**, 19023-19030.

11 W. Teng, N. Bai, Y. Liu, Y. Liu, J. Fan and W. X. Zhang, Selective nitrate reduction to dinitrogen by electrocatalysis on nanoscale iron encapsulated in mesoporous carbon, Environ. Sci. Technol., 2017, **52**, 230-236.